ORIGINAL PAPER - PRODUCTION GEOLOGY

Seismic reflection pattern and attribute analysis as a tool for defining reservoir architecture in 'SABALO' field, deepwater Niger Delta

Imoleayo Fashagba[1,2] · Pius Enikanselu[1] · Ademola Lanisa[3] · Olabode Matthew[4]

Abstract

An accurate definition of environment of sediment deposition is a sine qua non for characterizing and providing measures for enhancing hydrocarbon reservoirs. Consequently, this study is aimed at determining the sub-environment of deposition and architecture of two reservoirs: S1000 and S2000 reservoirs, in 'SABALO' field, deep offshore Niger Delta. In addition, the study is imperative in order to assess reservoir properties such as: geometry, connectivity and continuity, which are important for exploration and reservoir management. In this study, we integrated well logs from six (6) wells and 3D-seismic data (near and far angle stack) for seismic stratigraphic studies. Four major seismic sequences with their corresponding facies units were recognized by analysis of reflection terminations, seismic parameters and external geometry. The reservoirs of interest are within the seismic sequence one containing facies units: SF1A and SF1B. Both reservoirs were delineated to be structurally and stratigraphically controlled. This implies a combinational trapping system at the reservoir level. Also, hydrocarbons in the reservoir were confirmed to be down to reservoir base. Integrated study of the seismic and well logs shows that the two identified reservoirs, S1000 and S2000, were defined to be weakly confined channel complex with an area of 50 km^2 and 78 km^2, respectively. Their connectivity was defined to be loosely amalgamated and highly amalgamated, respectively. The results of this paper are essential to develop the reservoirs by utilizing the information of their geometry, connectivity and continuity.

Keywords Seismic facies · Attributes analysis · Reservoir architecture · Deepwater

Introduction

Over the past decade, there has been a significant rise in deep offshore exploration; however, this is presented with high risk and high cost (Bell et al. 2005; Skogdalen and Vinnem 2012; Reader and O'Connor 2014; Joye 2015). Therefore, it becomes imperative that exploration companies target and drill the right area where the prospects are located. In geologic context, deepwater implies sediment transport by gravity flow processes in a marine setting. The term 'sediment gravity flow' means the flow of sediment-fluid mixtures propelled by the influence of gravity. The flows can either be subaerial or subaqueous (Bouma 1964, 2004; Quiquerez et al. 2013). Other sedimentary processes such as rock fall, slumping and sliding also take place in deepwater (García et al. 2015). Sprague et al. (2005), integrated sequence stratigraphy, sediment delivery mechanisms and depositional processes to predict deepwater reservoir presence, distribution and quality in offshore West Africa. They asserted that the major determinant of reservoir type in deepwater slope and basin floor systems are: (1) the form of the sediment delivery system in regards to provenance, inland basins, shelf and shelf edge; (2) the flow type that generates at the shelf edge when sediments accumulate and finally become unstable; and (3) rugosity, gradient or physiography of the sea-floor. Traced from upslope and further into the basin, both modern and ancient deepwater environment of Niger Delta may be divided into the following end members (Fig. 1) defined by Sprague et al. (2005):

✉ Imoleayo Fashagba
   imolefashagba@gmail.com; imole@ankorpointe.com

[1] Department of Applied Geophysics, Federal University of Technology, Akure, Nigeria

[2] Ankor Pointe Integrated, Plot 27, Itummo Ogbonna Street, Lekki Phase 1, Lagos, Nigeria

[3] Total Exploration and Production, Victoria Island, Lagos, Nigeria

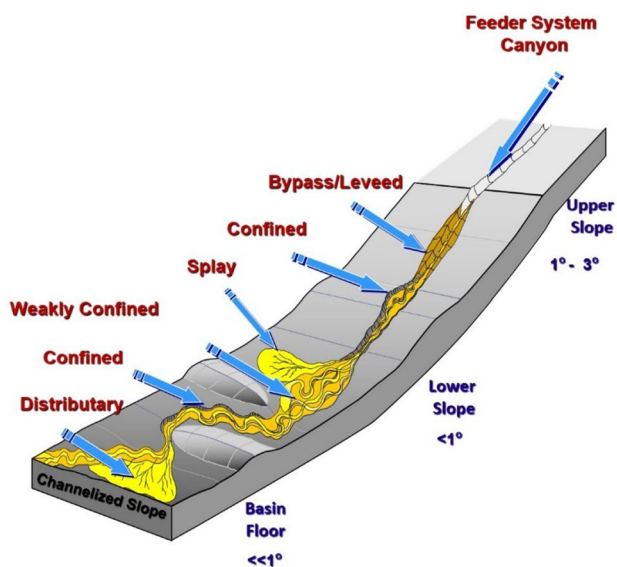[4] Sahara Energy Field Limited, Ikoyi, Lagos, Nigeria

Fig. 1 Deepwater depositional model and architecture in offshore, West Africa (Sprague et al. 2005)

1. Upper Slope (Bypass): Strongly erosional, muddy fill and very low net-to-gross.
2. Leveed Channel Complex: Aggradational overbank and splays, variable channel fill and moderate to low net-to-gross.
3. Confined Channel Complex: Strongly confined, complex erosional channel fill and moderate net-to-gross.
4. Weakly Confined Channel Complex: Lateral offset stacking, moderate to high net-to-gross.
5. Distributary Channel Complex: Mounded sheet like geometry laterally, amalgamated channels and high net-to-gross.

More detailed explanation of these deepwater depositional environments and architecture has been addressed by Posamentier and Kolla (2003), Olabode et al. (2010), Leffler et al. (2011), Moody et al. (2012), Chen (2012), Catuneanu (2012), Janocko et al. (2013), García et al. (2015), Xu et al. (2016), Zhang et al. (2017), Akinduluren et al. (2018), Deptuck and Sylvester (2018) and Tari and Simmons (2018).

In deepwater marine environment, one of such methods that helps to minimise prospect risk is to define the most likely sub-environment of deposition and reservoir architecture (Kahneman and Tversky 2013). A properly defined architecture forms the basis for understanding reservoir properties such as: geometry, connectivity and continuity, which are important for exploration, appraisal and reservoir management. Knowledge of this greatly improves reservoir development (Ofurhie et al. 2002; Grahame 2015; Bouroullec et al. 2017). The quest for seismic interpreters to understand the reservoir architecture leads them to carry out an integrated study. This kind of study, most times, requires integration of dataset such as: core, biostratigraphy, sequence stratigraphy, log motifs, thickness map and seismic facies analysis. The truth is that, we seldom have all this dataset to our disposal. And sometimes if the datasets are available, they may not cover the area of interest. In many cases, we are presented with well logs, seismic data and checkshots to work with. Over time, as the field is being developed, more datasets are added and become useful to comprehend the reservoirs.

One technique that proves to be a preliminary check for environment of reservoir deposition and its architecture is the concept of seismic facies analysis (Veeken 2006). The concept of seismic facies analysis is based on the fundamentals of seismic stratigraphy. First, seismic stratigraphic studies of a basin are done to delineate genetically related units, which are called seismically resolvable depositional sequence (Mitchum et al. 1977). Basically, the method for delineating depositional sequence boundaries is called the 'reflection termination mapping' technique (Vail 1977). Secondly, four major groups of seismic reflection distinguished in seismic sections (Veeken 2006) are: sedimentary reflections—representing boundary planes; unconformities or discontinuities in the geological record; artefacts—like diffractions, multiples, etc.; and non-sedimentary reflection like fault planes, flow contacts, etc. These seismic sequences are further described in terms of their configuration, continuity, frequency and amplitude. The description of the results produces a mappable, three-dimensional seismic unit composed of groups of reflections whose parameters differ from those of adjacent facies units (Mitchum et al. 1977).

Previous works such as those from Lanisa (2010), in his work titled 'Seismic Facies Analysis of Tertiary Deepwater Slope Deposits Lower Congo Basin, Offshore Gabon' and Jha et al. (2011), in their work titled 'Seismic and Sequence Stratigraphic Framework and Depositional Architecture of Shallow and Deepwater Postrift' have shown how seismic facies analysis can be used to describe architectural elements, morphology, and facies distribution of channel systems. The typical concept of seismic facies for reservoir architecture study has also been used by other authors (Shanmugam 2013; Alfaro and Holz 2014; Lehu et al. 2015; Olubola and Taiwo 2016; Amoyedo et al. 2016; Ndip et al. 2018; Okpogo et al. 2018); however, this paper presents a case study from deepwater Niger Delta, a region with growing studies. In our study, we present an integrated approach to define reservoir sub-environment of deposition and architecture in a case of limited dataset. This integrated Amoyedo technique involves the use of two seismic data class (near stack and far stack) and well data for seismic facies analysis and attribute extraction. Our study of 'SABALO' field addresses the problem of using seismic and well logs for predicting reservoir architecture in a case were data are not

sufficient to fully define reservoir sub-environment of deposition and architecture. In addition, it showcases a workflow that can be adapted for seismic facies analysis and attribute extraction for insightful definition of reservoir architectural properties. Furthermore, this research work presents a workflow that will help reduce uncertainties associated with defining sand fairway from amplitude extractions. Additionally, it describes how we can use sand fairway information to help reduce and minimize risk, thereby, allowing for much enhanced plans for mitigations and contingencies.

Field location and geological setting of the study area

The study area, 'SABALO' field, is located in deep offshore depobelt of the Niger Delta, Nigeria (Fig. 2a, b). Our study area lies within the transitional zone of the Niger Delta, which is characterised by a mix of normal faults and compressions. 'SABALO' field has a 3D-seismic data coverage of 251 km^2, the new name given to this field and the wells is only valid for this project.

The Cenozoic Niger Delta is situated at the intersection of the Benue Trough and South Atlantic Ocean, where a triple junction formed during the separation of the continents of South America and Africa in the Jurassic (Whiteman 2012). Consequently, the separation led to a subsidence of the African continental margin and cooling of the newly created oceanic lithosphere as separation continues into the early Cretaceous times. Further into the mid Cretaceous, a marine sedimentation took place in the Benue trough and the Anambra basin. And at the onset of the Tertiary times, the Niger Delta started to evolve as a result of increase in river clastic input (Doust and Omatshola 1989). Presently, the delta spreads through the Gulf of Guinea (Ahlbrandt et al. 2005). The units of the steps of the outbuilding sediments in the Niger Delta formed depocenters within the delta, which are successive phase of the delta growth. Depocenters (also known as depobelts) are now known to consist of bands of sediments about 30–60 km wide in lengths of up to 300 km, they are also bounded by major faults (Obaje 2009). Structurally, the delta features a large presence of syn-sedimentary growth faults, shale diapirs and rollover anticline which deformed the delta complex (Evamy et al. 1978). Also, rollover anticlines form a greater percentage of the fields in the delta.

Since the Palaeocene, the delta has prograded a distance of more than 250 km from the Benin and Calabar flanks to the present-day delta front (Evamy et al. 1978). The delta has an average thickness of 12 km which covers an area of about 140,000 km^2 (Doust 1990). Overall, the deformation within the delta is grouped into three categories: extension, translation and compression zones. The area of interest is within the transition zone of the delta (Fig. 2a).

Stratigraphy and petroleum geology

Palynomorphs and foraminifera zones form the key basis for the correlation of stratigraphic framework of the Niger Delta (Obaje 2009). Fundamentally, there are three broad lithostratigraphic units, from the oldest to the youngest: Akata Formation (a basal marine shale unit underlying the entire delta and usually overpressure), Agbada Formation (Coastal marine sequence of alternating sand and shale) and Benin Formation (recent sequence of shallow
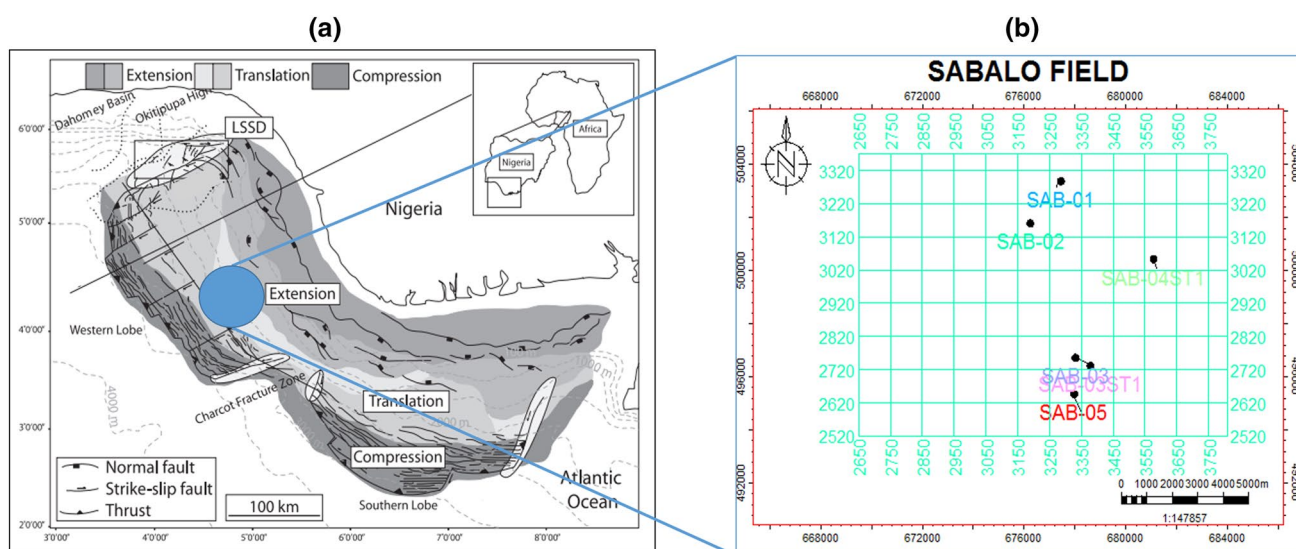

Fig. 2 Map of offshore Niger delta. **a** Structural Domains in Niger Delta (Modified after Leduc et al. 2012). **b** Base map of the study area showing well locations

marine sands). The nomenclature of the delta shows an overall upward transition from marine shales through a sand-shale paralic interval to continental sands. (Doust and Omatshola 1989) estimated that the Akata formation about 7000 m thick. Agbada Formation is over 3700 m thick, and the recent Benin Formation is up to 2000 m thick.

In the Niger Delta, there has been only one petroleum system recorded, and this is the Tertiary Niger Delta (Akata-Agbada) petroleum system. The source rock has two variable contributions from the Akata Formation and interbedded shale in the lower Agbada Formation, which is in similarities with the marine Akata Formation. Turbidities sand at the top of the Akata Formation are potential reservoirs in deep water because the Akata Formation formed during lowstands when terrestrial Structural traps have been the most favourable exploration targets. However, stratigraphic traps are likely to become more important targets in distal and deeper portions of the delta. The structural traps developed during syn-sedimentary deformation of the Agbada paralic sequence (Evamy et al. 1978; Stacher 1995).

Materials and methods

In this study, we integrated well logs and 3D-seismic data to delineate reservoirs and carry out seismic facies analysis. The field was interpreted with the aid of Petrel E&P software. In addition, Microsoft Excel was used basically to build a polynomial function; this function serves as a direct velocity model used for time depth conversion of mapped surfaces.

Our interpretation workflow starts with quality check (QC) of both seismic, well log and checkshot data, followed by well log correlation. Then, sonic calibration for assessment of the both sonic and checkshot data and generation of a time-depth relationship models were applied for the seismic–well tie process. Afterwards, the well tops identified on the well logs are tied to their corresponding events on seismic by doing a seismic-to-well tie for all the wells. Structural interpretation (mapping of faults and horizons from vertical seismic sections) and depth conversion were then carried out. A key aspect of the workflow then followed; this is the definition of stratigraphic framework by carrying out seismic stratigraphic analysis and identification of seismic facies. This was done by using the concepts described in "Introduction" section. A similar approach to the facies description is adopted from the three authors: Posamentier and Kolla (2003), Lanisa (2010) and Jha et al. (2011). Finally, the reservoir architecture along with parameters such as geometry, connectivity and continuity was defined.

Results and discussions

In this study, we have determined the sub-environment of deposition (EOD) and architecture of two reservoirs of interest (S1000 and S2000), and from this, we inferred their geometry, connectivity and quality. The results and discussions are in presented in a sequential order. Results are presented as maps, sections and correlation panels.

Identification of reservoirs

Foremost, reservoirs were identified in the SAB-01 well (this is the exploratory well drilled in the field). Five reservoirs (Fig. 3) were identified within 'SABALO' field, and they include; S1000, S2000, S3000, S4000 and S5000. The reservoirs of interest are the S1000 and S2000 reservoir. Qualitative analysis of the well logs indicated that the S1000 reservoir has an inherent log issue at the SAB-01 well (Fig. 4).

The gamma ray log interval within 7800–7850 ft shows the presence of sand; however, it does not represent the true formation reading due to the straight line, and when juxtaposed with the neutron-density log (highlighted by the orange circle in Fig. 4), it indicates that the interval is shale, which is contrary to what is seen on the gamma ray log. As a result of this issue, the top of this reservoir could not be defined. However, the base of the reservoir was determined to be at depth of 7893 ft. This issue was well noted for further evaluations carried out in the study. The top of S2000 reservoir is at an approximate depth of 8000 ft and
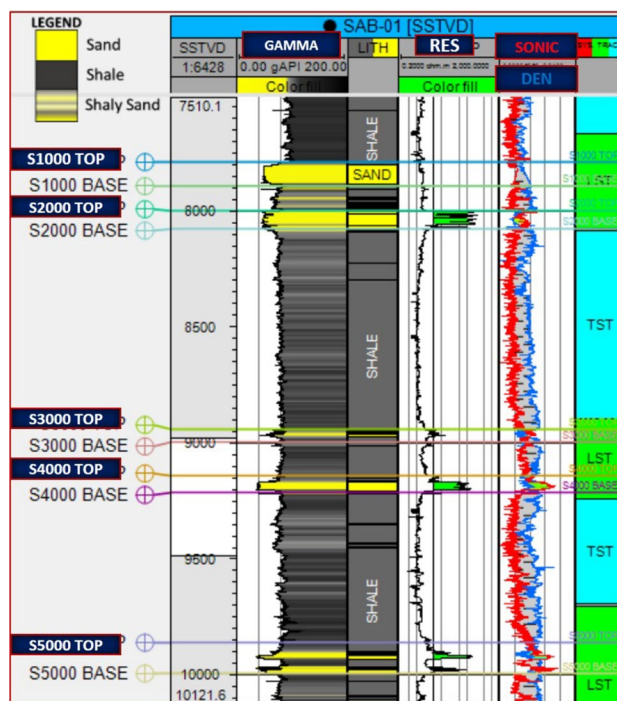

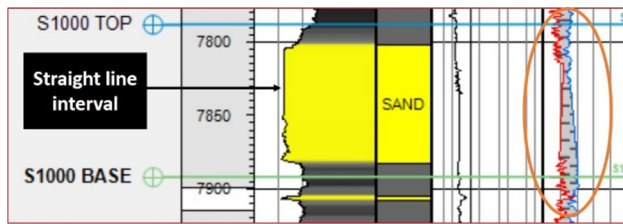**Fig. 3** Reservoirs identified in SAB-01 well of 'SABALO' field

Fig. 4 Well log section of SAB-01 well, showing issues with S1000 reservoir

the base of the reservoir is at 8077 ft. In this reservoir, the approximate thickness was about 77 ft. Furthermore, qualitative analysis of the neutron–density logs showed that S1000 reservoir is observed to contain water, while the S2000 reservoir contains hydrocarbon in the SAB-01 well. The fluid types were interpreted using the neutron and density logs. The lithology was defined on the basis of using gamma ray logs, and other auxiliary logs such as caliper and neutron-density. The hydrocarbon contained in these units of reservoirs is down to the base of the reservoir. This is described as Oil-Down-To (ODT).

Vertical seismic resolution

Tuning thickness was estimated from the six (6) wells present in 'SABALO' field. This was established by using the Widess vertical resolution model of lambda divided by 4 ($\lambda/4$), where lambda is the wavelength (Widess 1973). Tuning starts to occur below the vertical resolution, and thus, reflections start to have partial interference. The partial interference range is defined to be the detectability limit of the seismic data. The dominant wavelength of these reservoirs was defined using the relationship between average interval velocity (v), dominant frequency (f) and dominant wavelength (λ), which is an approach by Simm et al. (2014). The estimated average vertical resolution of the seismic data for thick bed response using the equation proposed by Widess (1973), is 93 ft or 28 m (Table 1). Also, the average detectability limit is defined as 46 ft or 14 m (Table 1). Basically, it implies that any reservoir below the thick bed response would be detectable because they fall within the detectability

range; however, it will be poorly resolved on seismic data. Within the detectability range, there would be partial interference of the reflection from the top and base of the reservoir. Beyond the detectability limit, the response seen on seismic data will not be a true response due to destructive or constructive interference of the reflections from the top and base of the reservoir building up to amplitudes of smaller or larger values, respectively. This region is known as maximum interference (Fig. 5).

To extract reliable seismic attributes for characterization, it is always vital to establish that the reservoirs are either above tuning thickness or closely detectable on the seismic data. As shown in Fig. 5, it is observed that much of the reservoir thicknesses are in the partial interference zone, except for the S1000 reservoir in the SAB-04ST1 well. While this may not give us a perfect resolvability, it can still serve as a guide to understand our reservoir with attribute extractions, given proper calibration of the well-to-seismic data.

Lithostratigraphic correlation

A well correlation was carried out in order to define the lateral extent of the reservoir of interest identified on the SAB-01 well. Results for the S2000 and S1000 reservoir correlation using the six wells in 'SABALO' field (from SAB-01 well to SAB-05, over an interval of 13,730 m) are shown in Fig. 6. The concept of sequence stratigraphy, comparison of shale packages and resistivity markers were the standards used for well correlation. Our observations were that the S2000 and S1000 reservoirs are two sequences of sands separated by a shale unit. The sands are seen to be extensive and show varying thickness through the interval covered by the wells. The S1000 reservoir is thickest in SAB-04ST with a thickness of about 190 ft. The reservoir thins out towards SAB-02 and SAB-05 well to a thickness of about 30 ft and 40 ft, respectively.

While the correlation shows that the reservoirs have varying thickness, however, the S2000 reservoir does not show exactly the same thickness variation with S1000. S2000 shows appreciable thickness of 170 ft, 60 ft and 80 ft in SAB-01, 04ST and 05 wells, respectively. The reservoirs thin out in SAB-02 and -03ST well to a thickness of 35 ft

Table 1 Estimated seismic resolution at $\lambda/4$ (thick bed response) and $\lambda/8$ (partial interference)

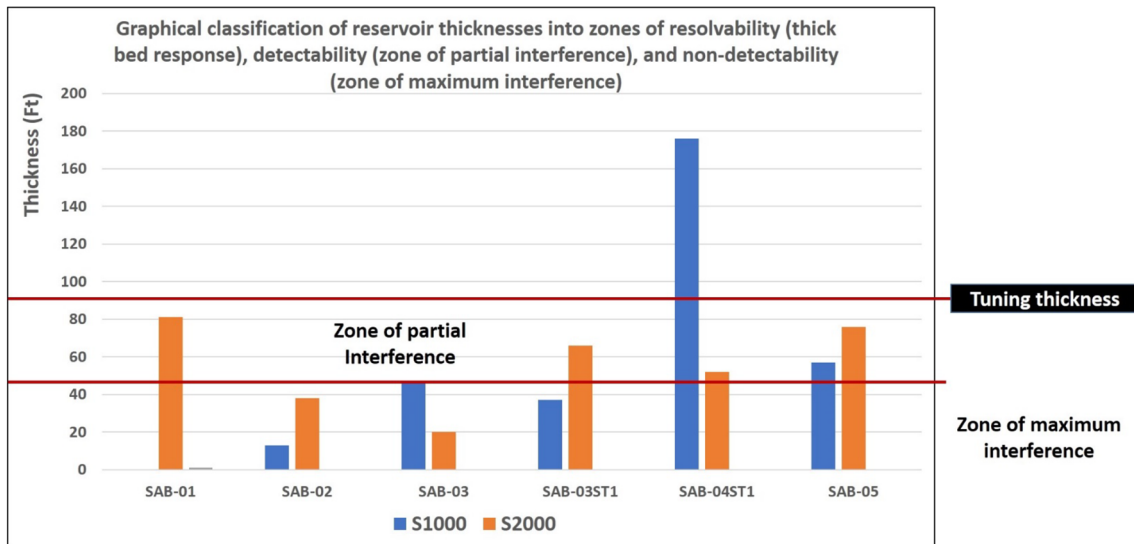| Well	Dom. frequency (Hz)	Av. velocity (ft/s)	Wavelength (ft)	Tuning (ft)	Tuning (m)
SAB-01	23	7194	312.8	78.2	23.8
SAB-02	20	7752	387.6	96.9	29.5
SAB-03	21	8032	382.5	95.6	29.1
SAB-03ST1	21	8620	410.5	102.6	31.3
SAB-04ST	22	8000	363.6	90.9	27.7
SAB-05	21	8065	384	96	29.3

Fig. 5 Graphical classification of reservoir thicknesses into zones of resolvability, detectability and non-detectability
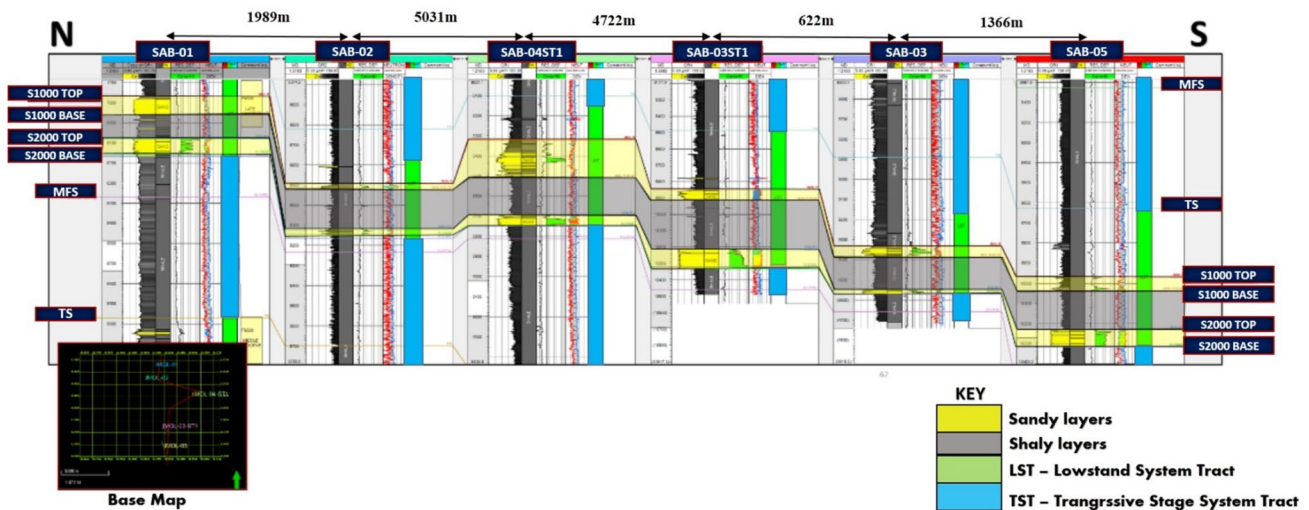

Fig. 6 Litho-stratigraphic correlation of wells in 'SABALO' Field

and 30 ft, respectively. Overall, most section of the reservoir thicknesses are within the partial interference zone (Fig. 5), which proves that they could detectable on the seismic data.

Seismic-to-well tie

After the well correlation, a synthetic seismogram was generated by convolution of a zero-phase wavelet and the reflection coefficient series. The seismic-to-well tie was done in order to ascertain the correct horizon to pick for reservoir interpretation. Figure 7 shows the seismic-to-well tie carried out for SAB-01 well. First, a sonic calibration was carried out in order to combine the accuracy of the check shot

data with the detail of the sonic log to get the best possible time–depth relationship (TDR). The new TDR becomes active for the well, and it was used for the synthetic generation process. Then, the SAB-01 well (and other wells) was tied to the near-stack seismic data. This is because a compression sonic was used for the synthetic generation process and it only accounts for primary incident wave (P-wave), and the only seismic data stack that is closest to fully account for the P-wave is the near-stack seismic data. A zero-phase 21 Hz Ricker wavelet with normal polarity was used for the convolution. The frequency of this ricker wavelet was estimated from the seismic data within the reservoir of interest. A zero-phase Ricker wavelet was utilized because the
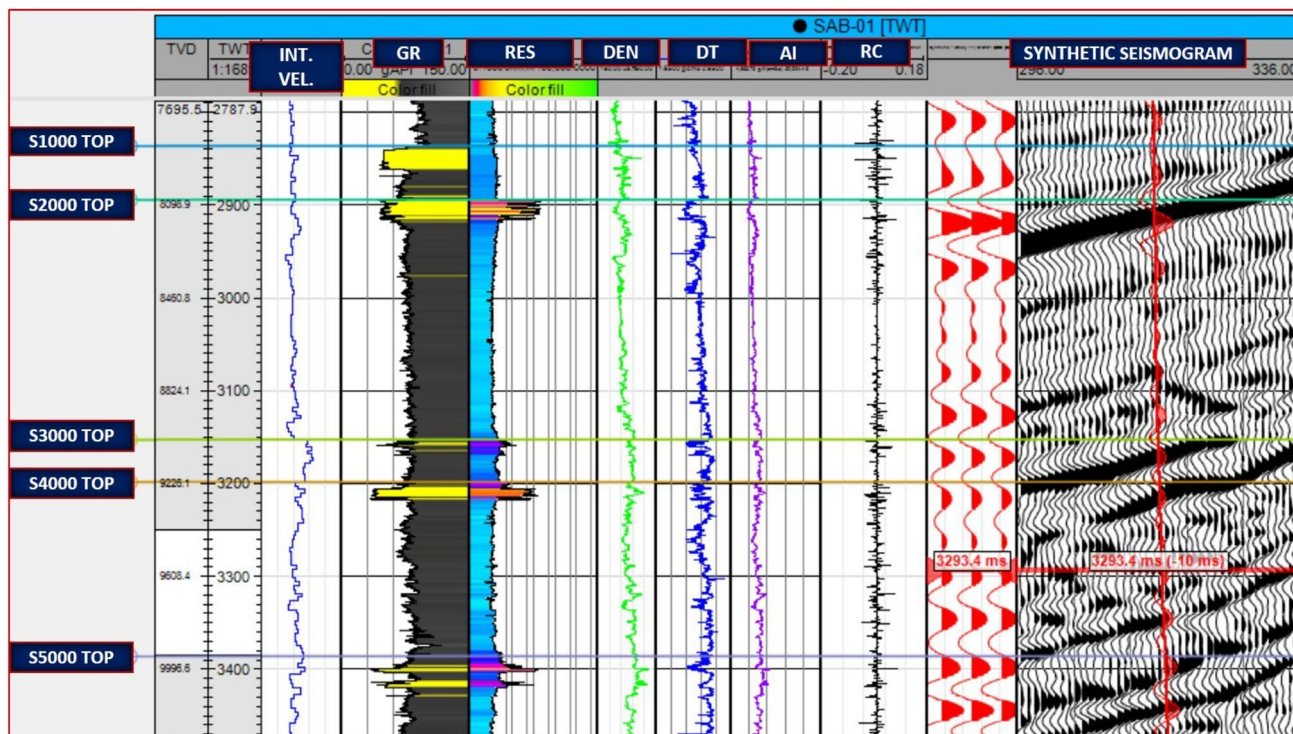
Fig. 7 Well-tie for SAB-01 well, where the displayed logs are: interval velocity (INT-VEL), gamma ray log (GR), resistivity log (RES), density (DEN), sonic log (DT), acoustic impedance (AI), reflectivity log (RC) and synthetic seismogram. In the last track, the generated synthetic seismogram is overlain on the original seismogram for visual comparison

information accompanying the dataset indicated that the seismic data are in zero phase. Overall, the result shows a good tie as a bulk shit of -10 ms was done to tie the synthetic to the seismic data. The bulk shift was done in order to match the geologic response of the synthetic seismogram and the seismic data. From the well tie carried out, it was seen that the top of the reservoirs of interest corresponds to a trough and this implies that they are low-impedance sand overlaid by high impedance formation shale. After successful completion of the well tie for SAB-01 well, all other wells were tied to the seismic data. Similar polarity of seismic data was observed on all other well ties for the reservoirs of interest.

Furthermore, we validated the polarity and phase of the seismic data using the seismic reflection from the seabed (Fig. 8). It was noticed that the seismic reflection from the seabed corresponded to a peak. Since the seabed is a region of higher impedance than the water interface, then we can safely conclude that for the seismic data: Peak implies high impedance shale, while trough implies low-impedance sand.
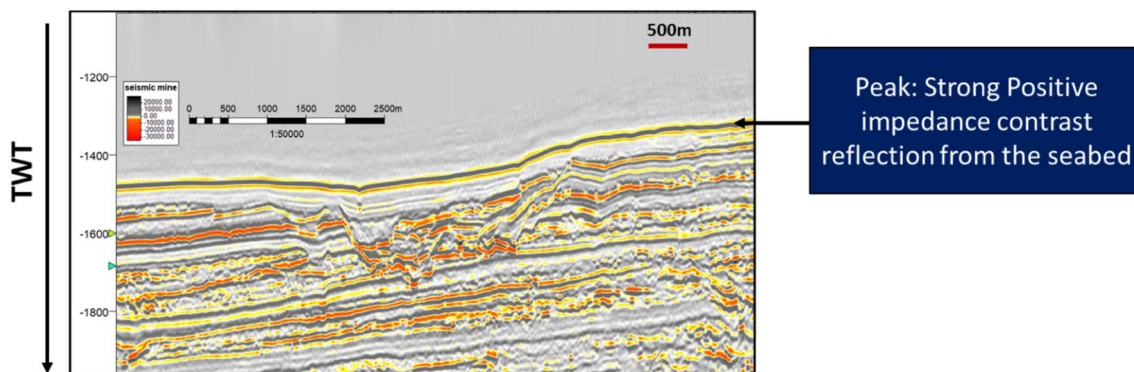

Fig. 8 Seismic reflection from the seabed indicating SEG positive standard polarity and zero phase for the seismic data

Seismic facies analysis

Seismic sequence and facies identification

In our study, four (4) major sequences (Fig. 9a, b) were observed in this field by analyses of the reflection terminations (onlap, toplap, downlap and truncation) and observation of seismic reflectors in terms of their amplitude, continuity, configuration, frequency and corresponding external geometries (tabular, lenticular, mounded, wedge, etc.). Each of these seismic sequences is then further sub-divided into two seismic facies after analysing their characteristics. From the well-to-seismic tie carried out, it is observed that sequence of interest (i.e. the sequence containing S1000 and S2000 reservoir) is sequence 1. Observations for each sequence are described below.

Seismic Sequence 1 This interval is the bottom part of the seismic data (Fig. 9a) to a range of about −3252 ms (i.e. from the bottom part to the blue line in Fig. 9a, it is also represented in Fig. 9b from the bottom to the brown line). This is controlled by post-deformations as a result of mobile shale diapirism. Reflection in this sequence displays parallel internal configurations being concordant to the sequence boundaries. This sort of configuration indicates unique form sedimentation conditions for an infill or a sequence on top of subsidising substratum (Veeken 2006). This geometry in deepwater reflects a bottom set situation. Two seismic facies unit were identified within the sequence, namely Facies SF1A and Facies SF1B.

Facies SF1A These units are reflections with low to medium values of amplitude, low values of frequency and high continuity (Fig. 9b). They indicate more similar lithologies on both sides of the interface (e.g. silty shale or shale), based on frequency and continuity observations this is interpreted to be bed intervals (i.e. shale prone, or sediment starved areas in deepwater). This unit is interpreted as areas of non-erosive fill, indicating basin floor topography with areas of starved sedimentation, shale filled and subsequently flattened out by further infill.

Facies SF1B These are reflections (Fig. 9b) also showing parallel internal configurations, but with high amplitudes being discontinuous (i.e. low continuity) with medium frequency. This is interpreted to be either sheet sands or weakly confined channels.

Seismic Sequence 2 This sequence (Fig. 9a, b) is less continuous and undisturbed with evidence of erosional truncation at the top, observed internal configurations are parallel with presence of external geometries. Two seismic facies have been identified in this sequence. The sequence extends from about −3250 to −2240 ms (i.e. blue line to black line in Fig. 9a and brown line to orange line in Fig. 9b).

Facies SF2A These facies (Fig. 9a, b) are wedge-shaped erosive within the parallel internal configuration with low to medium values of amplitude, interpreted to be erosive channel and its fill forming channel levee overbank complex. This also has medium to high values of frequency as
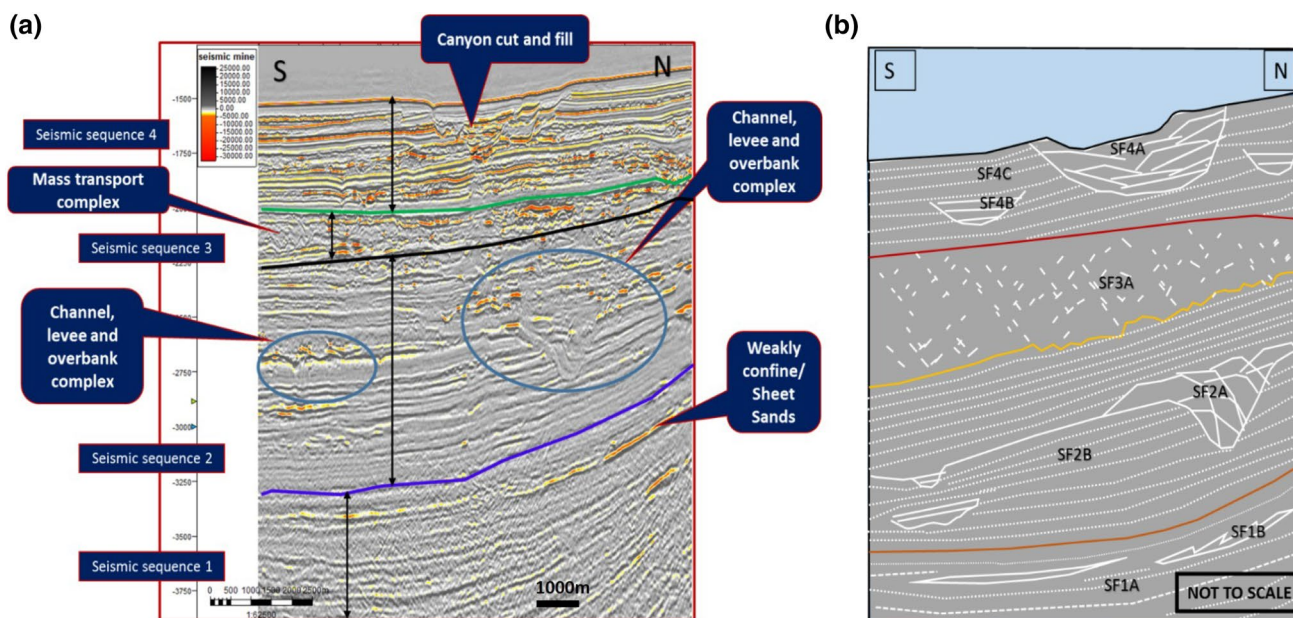

Fig. 9 An interpreted generalized seismic section for seismic sequence and facies analysis. **a** Interpreted section for seismic sequence analysis of 'SABALO' Field. **b** Schematic image illustration of facies unit identified within each sequence

bed thickness increases. It is observed that the facies show an erosive fill indicative of lateral change in energy level, with an oblique (lateral accretion) and vertical aggradation geometry.

Facies SF2B These are reflections are similar to the SF1A facies. It consists of parallel internal configurations with low to medium values of amplitude and low to medium values of frequency. They indicate more similar lithologies on both sides of the interface (e.g. silty shale or shale).

Seismic Sequence 3 This sequence extends from about −2240 to 2000 ms (i.e. the black to green line in Fig. 9a and from the orange to red line in Fig. 9b) is a chaotic and disturbed sequence overlying and onlapping on sequence 2. One seismic facies unit is defined in this sequence.

Facies SF3A These are facies (Fig. 9a, b) with high to medium amplitude coupled with discrete continuities and variable frequency. This usually suggests a highly disturbed internal organization of the deposits. This signature could be observed in all kinds of depositional environment. However, for the case of deepwater study, one can safely conclude that they are mass transport complex/gravity flow of mud.

Seismic Sequence 4 This is the topmost seismic sequence from the −2000 ms to the top at about −1400 ms (i.e. from the green line to the top in Fig. 9a, and from the red line

moderate to high amplitude and low to moderate continuities. Two seismic facies have been identified in this sequence, SF4A and SF4B.

Facies SF4A This is a U-shape with parallel reflections, and erosional features interpreted as recent canyon cut and filling stage, this has a frequency range drastically changing which are as a result of individual filling stage of the canyon. The geometry also displays vertical aggradation (Fig. 9a, b). A depth seabed map shows the canyon geometry, and the trend is displayed in Fig. 10a. This is further enhanced using the variance attribute time slice (Fig. 10b) which shows how different channels have migrated through the canyon cuts into one another.

Facies SF4B This (Fig. 9a, b) indicates the presence of other few and small channel geometries with low to medium frequency and short continuities.

Facies SF4C This unit (Fig. 9a, b) defines the non-erosive fill of sequence 4. It indicates area of starved sand sedimentation and as a result being shale filled.

Interpretation of observed seismic facies pattern

The seismic facies analysis clearly defined depositional trend of the deepwater basin. It clearly shows the prograding nature of the Niger delta basin. The interpreted facies
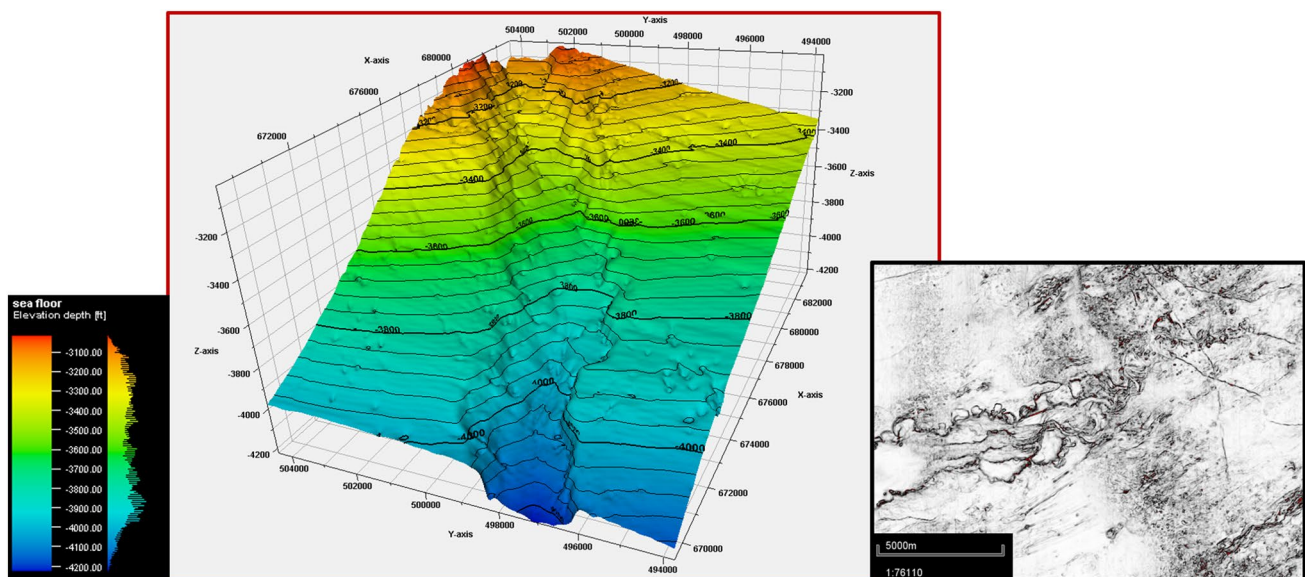

Fig. 10 Canyon geometry and channel trend. **a** Depth map of the seabed. **b** Variance time slice attribute from the seabed showing channel trend along the canyon

to the top in Fig. 9b). By scanning through the data, this sequence occasionally displays bright reflections generally

unit from the seismic section (Fig. 9b) shows sequence one (1) to sequence four (4). Each phase of the sequence marks

further infill and shift in facies (regression) into the basin. Hence, more sediment is brought into areas that were previously starved of sedimentation. The story builds up from an area that is once the basin floor, where submarine fans form (Sequence 1) to an area marked by farther regression (Sequence 2), with evidence of channel–levee complex systems occurring at higher relief, slope and then followed by mass transport deposits (Sequence 3) to the recent canyon cut and fill stage feeder input system (Sequence 4) for sedimentation meaning at this present stage sediment have travelled further into the basin.

Qualitative amplitude assessment

In order to make sense of what could have been responsible for amplitude variation with offset (AVO), seismic amplitudes were qualitatively inspected in S1000 and S2000 reservoirs. A section was taken across SAB-03ST1 well, which had the same well head as SAB-03. In Fig. 11a, it is seen that S1000 and S2000 reservoirs are hydrocarbon bearing in SAB-03. The S2000 reservoir is also hydrocarbon bearing in SAB-03ST1 well. However, S1000 reservoir was found to be brine in SAB-03ST1.

As earlier established from seismic-to-well tie, the tops for both reservoirs correspond to a trough (orange colour on the seismic section). On the near stack, it was observed that the tops of both hydrocarbon and non-hydrocarbon bearing

Fig. 11 Seismic section across SAB-03ST1 and SAB-03 well. **a** Near-stack seismic section showing wells and reservoirs top. **b** Far-stack seismic section showing well and reservoir tops
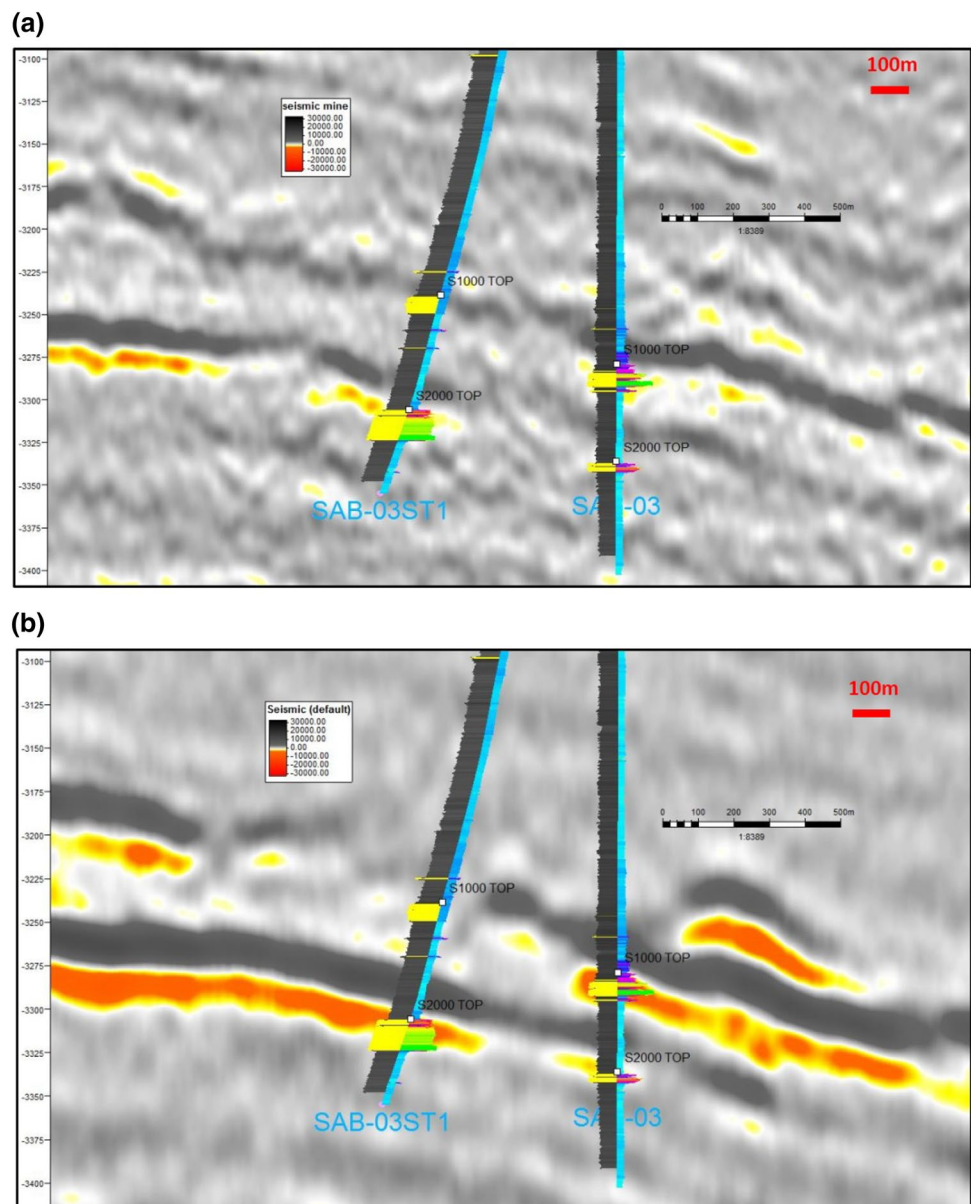
reservoirs ties to a trough (Fig. 11a). However, an increase in amplitude with offset was observed in only the hydrocarbon bearing reservoirs (Fig. 11b), thus indicating a class 3 AVO, which could be largely due to fluid effect.

Seismic attribute: minimum amplitude extraction

The second phase of seismic facies analysis involved the use of seismic attributes to reveal subtle features in the seismic data. The following results are discussed.

Near-stack minimum amplitude extraction For near stack, the angle of incidence is almost at zero offset, and the resulting amplitudes extracted can be used for defining environment of deposition of a reservoir (Brown 2011). Minimum amplitude extraction from the reservoir surface shows the distribution of amplitudes on the surface. This distribution is related to sand fairways over the surface, as high or bright amplitudes (trough; negative amplitude) correspond to regions with sands, while regions of low amplitudes correspond to regions with less sand or shale. Near amplitude extractions for S1000 and S2000 (Figs. 12a and 13a) reservoir top show the distribution of sand and shale on the map, and the form which they take is typical of what is observed in a weakly confined channel environment, thus making it a vital information for defining the environment of deposition for S1000 and 2000 reservoirs.

Far stack minimum amplitude extraction Results for both S1000 and S2000 reservoir top are displayed in Figs. 12b and 13b respectively. The reservoirs show characteristics of class 3 AVO (Amplitude Versus Offset), whereby amplitude negatively increases further with offset. This confirms regions possibly containing hydrocarbon in the area.

Log motif (signature) map, isopach map and NTG integration

As earlier described in "Introduction" section, the reservoir sub-environment of deposition and architecture requires an integrated approach in order to affirm the results and properly define our interpretation. While observations made from the attribute extractions (see "Seismic attribute: minimum amplitude extraction" section) may not be sufficient to clearly define the channel architecture, however, a qualitative check (see "Qualitative amplitude assessment" section) was done on the seismic data by observing how the response in a brine sand and the response in an oil sand. We could see that changes in amplitude were only observed in the oil sand, and this clearly showed that the far-stack data was responding to fluid effects. In order to vet that the response from the near-stack seismic data was mainly as a result of lithology, an

integration of the True Stratigraphic Thickness (TST) map, log motif and net-to-gross ratio was done.

In order to affirm and quality check results from the amplitude extraction, log motifs (Fig. 14) for the reservoirs of interest were posted on the reservoir top surface map. The log motifs of the reservoir intervals are typically more of middle fan channel (see log motif beside maps) for the S1000 (Fig. 12a), and the S2000 (Fig. 13a) reservoir. Displaying the reservoir interval from the well log on the surface maps helps to give an idea of how the net sand thickness correlates to amplitudes extracted onto the surface map. Although, this was done with consideration of the tuning thickness of the reservoirs in each well and that the gamma ray log of the S1000 reservoir in SAB-01 well is not a true representation of the reservoir information as described in "Identification of reservoirs" section. In most part, the reservoirs are in the range of detectability, except for reservoir thicknesses in SAB-02 and SAB-03 well (Fig. 5). With this in mind, we carefully correlated the seismic amplitudes to log motifs. The results show good conformance to the distribution of sand fairways identified on the near-stack amplitude extraction map described earlier in "Interpretation of observed seismic facies pattern" section. The regions where the well intersects the bright amplitudes (i.e. regions interpreted to be sand) show the presence of sand on the gamma ray logs (especially for regions with appreciable detectability on seismic) and areas where it intersects the dim amplitudes (i.e. regions interpreted to be shaly zones) show the presence of shale on the gamma ray logs. Also, there is a good conformance between the far stack amplitude extraction map described in "Interpretation of observed seismic facies pattern" section. The areas on the far amplitude map that intersects the wells were interpreted to be an oil-down-to (ODT) reservoirs; consequently, this affirms the result of the well correlation. Overall, both channel complex as observed from seismic facies, amplitude extractions and log motifs are seen to be constructive with S1000 having elements of moderate net sand richness compared to S2000 with a higher net sand richness. The Isopach map for the S1000, and S2000 are shown in Figs. 15 and 16, respectively. The maps show the distribution of the true stratigraphic thickness over the surface area. Areas of high stratigraphic thickness (i.e. regions of southeast to southwest of the S1000 reservoir in Fig. 15 and the regions of the northeast and southeast of the S2000 reservoir in Fig. 16) conform to areas of high amplitude on the near-stack minimum amplitude extraction map (this is described in "Seismic attribute: minimum amplitude extraction" section). Furthermore, appreciable thickness between 80 and 100 ft observed around the channel axes are similar to what was identified on the litho-correlation for both reservoirs (see "Lithostratigraphic correlation" section). These results confirm the possibility that the environment of deposition as earlier identified are what they are.
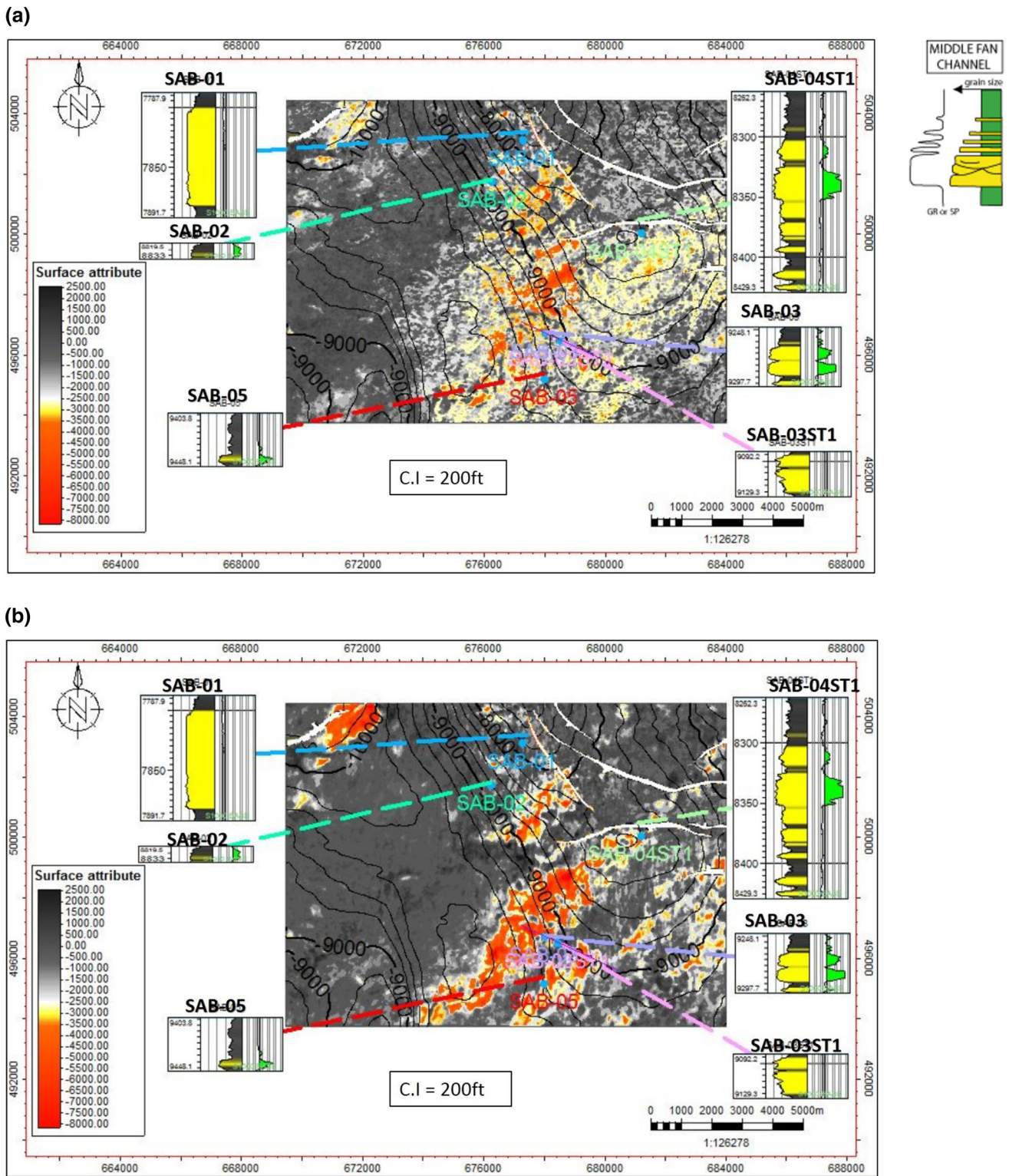
(a)

(b)

Fig. 12 a S1000 reservoir top near-stack minimum amplitude extraction map overlaid with log motif from the each wells. **b**: S2000 reservoir top far stack minimum amplitude extraction map overlaid with log motif from the each well. C.I. means contour interval
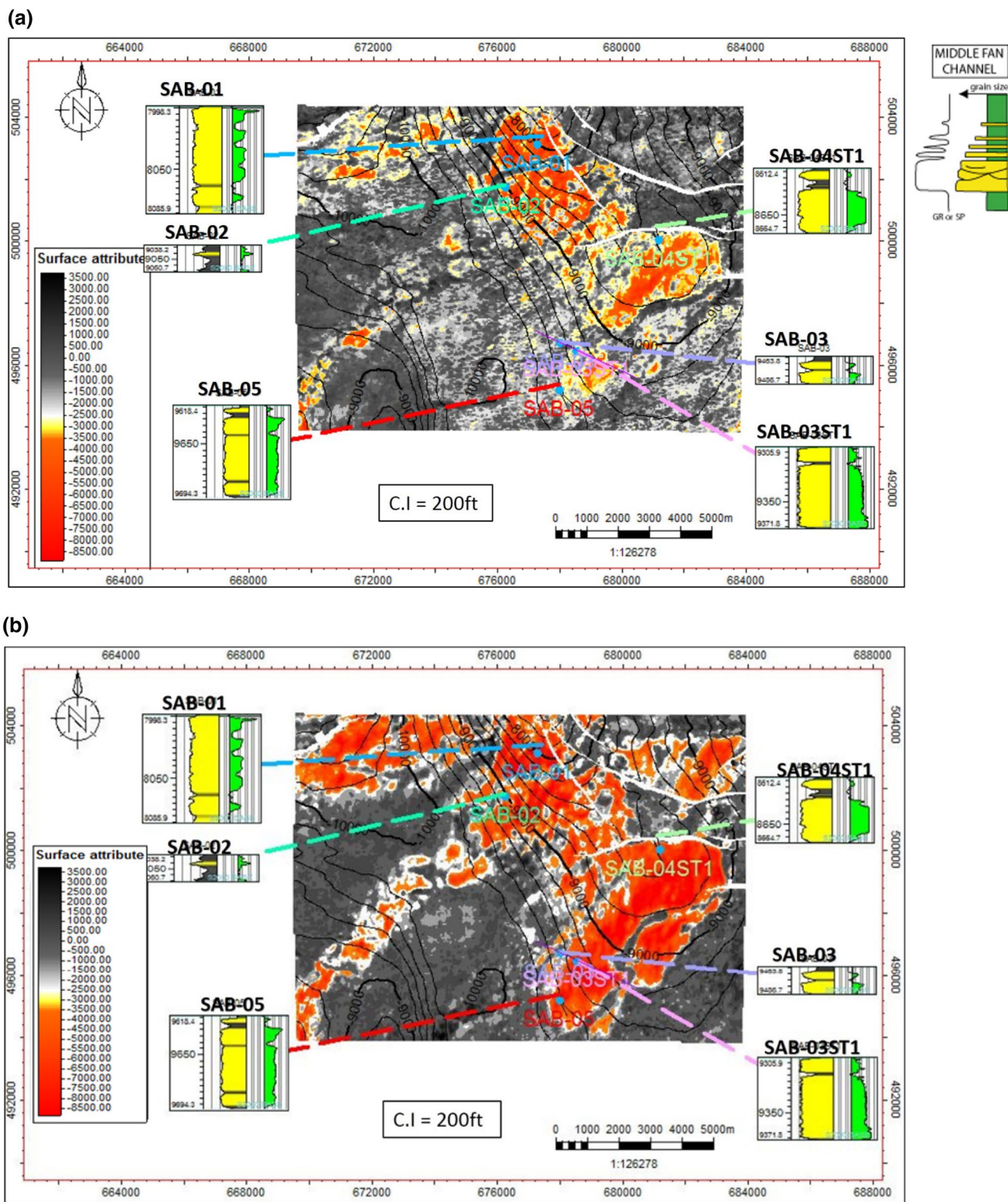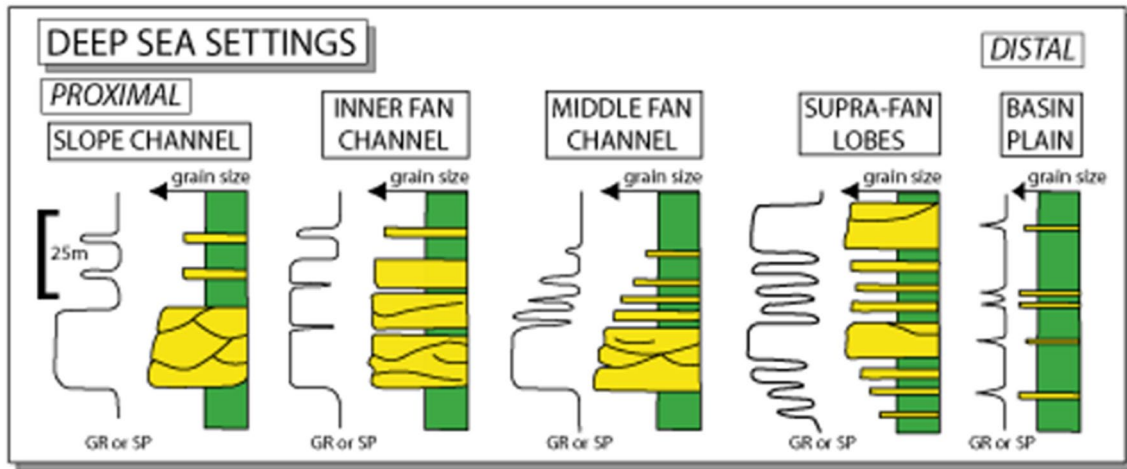
Fig. 13 **a** S2000 reservoir top near-stack minimum amplitude extraction map with log motif from each well. **b** S2000 reservoir top far stack minimum amplitude extraction map with log motive from each well. C.I. means contour interval
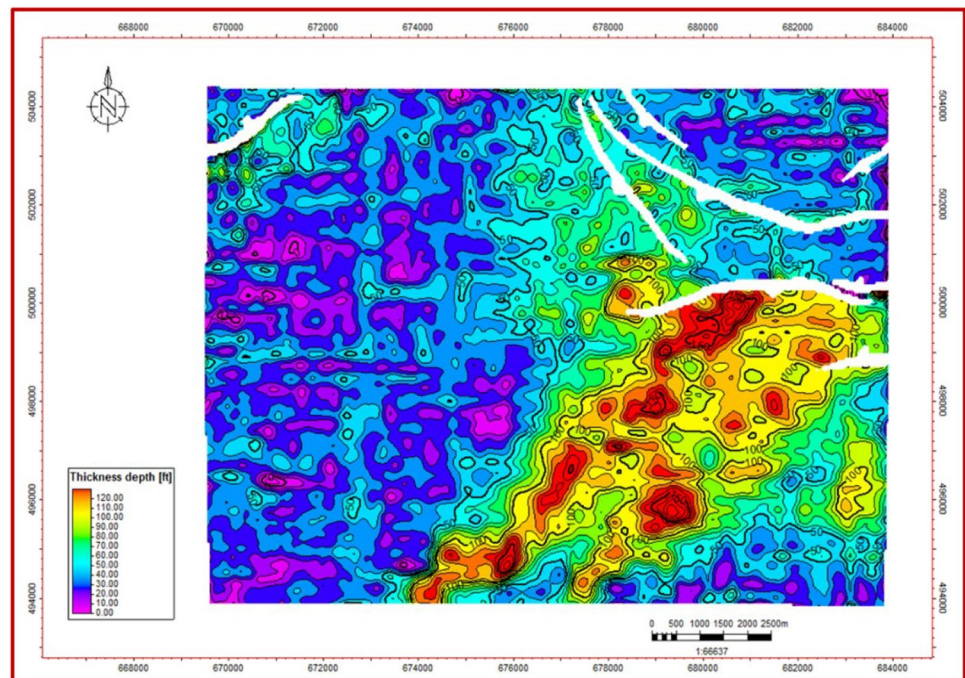
Fig. 14 Log motifs of depositional environment in deepwater settings (modified from Rider 1999)

Fig. 15 True stratigraphic thickness (TST) map of S1000 reservoir

The TST map conforms with the near-stack minimum amplitude extraction map and reservoir thickness from log motif. It was observed that the TST map took a form corresponding to the sand fairway observed in the near-stack amplitude maps. Secondly, the log motif for each well on the amplitude map (Fig. 12a, b) helped to confirm the possible sand fairways interpretation, which are regions with bright amplitudes (red to orange colours) on the near-stack amplitude map. These regions tied to where we had an appreciable sand thickness on the log.

To further validate the sand fairways, the NTG from each of the reservoirs were computed (Table 2). The result of S1000 reservoir shows NTG in the range of 0.14–0.91, with SAB-02 well having the lowest NTG and SAB-04ST1 having the highest NTG. For S2000 reservoir, the NTG ranges between 0.11 and 0.87, with SAB-02 well having the lowest NTG and SAB-01 having the highest NTG. It was observed that regions of high NTG values of 50 and above correlates to regions of inferred sand fairways from the amplitude and TST map. Similarly, regions of low NTG correlate to shaly regions on the near-stack minimum amplitude extraction map (Fig. 12a, b). Overall, integrating seismic reflection patterns, log motives, TST and NTG maps, we were able to make an informed inference about the sand fairways,

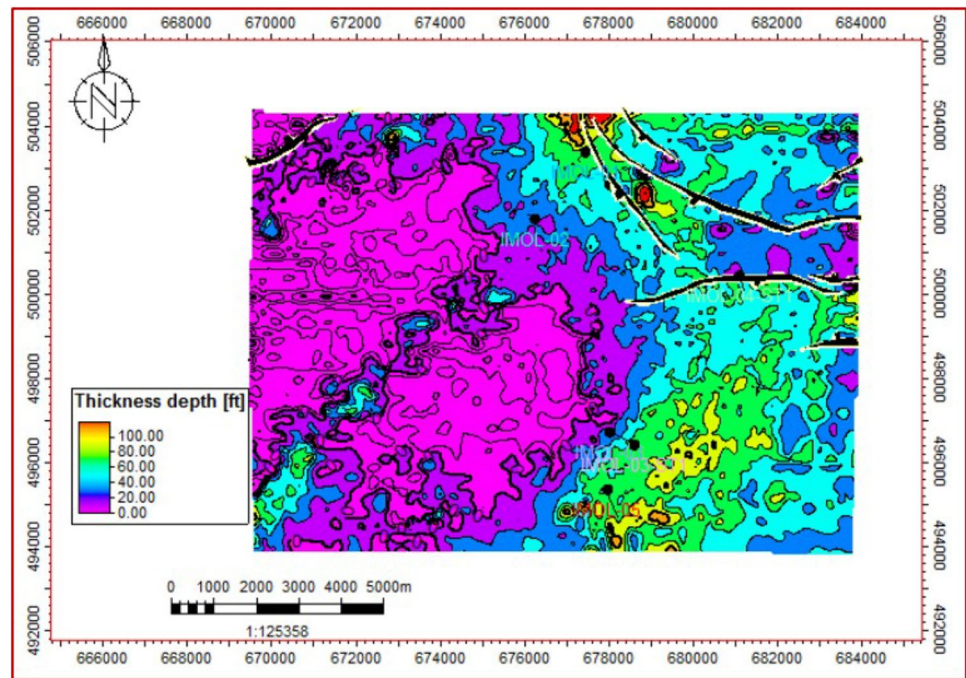**Fig. 16** True stratigraphic thickness (TST) map of S2000 reservoir

Table 2 Estimated NTG from S1000 and S2000 reservoirs

Wells	S1000			S2000		
	Top (MD)	Base (MD)	NTG	Top (MD)	Base (MD)	NTG
SAB-01	7867.52	7971.27	Nil	8077.9	8165.47	0.874
SAB-02	8901.3	8914.83	0.144	9120.03	9142.58	0.11
SAB-03	9190.11	9378.92	0.856	9393.47	10,331.93	0.696
SAB-03 ST1	9847.07	9909.21	0.868	10,209.9	10,332.1	0.912
SAB-04 ST1	8343.16	8510.25	0.91	8693.63	8745.95	0.807
SAB-05	9982.3	10,033.14	0.23	10,227.82	10,314.32	0.84

ultimately helping us to refine our knowledge of the possible sub-environment of deposition of the channels, their channel axes, off axes, margins and possibly their architecture.

Reservoir geometry and connectivity: an assessment for reservoir development and management

Definition of geometry of the reservoir involved the definition of the size, shape (structure), area and trend of reservoirs. The structure of the S1000 and S2000 reservoirs was interpreted to be controlled by a faulted crest anticline core with a saddle separating the western and eastern highs (Fig. 17a, b). The anticlinal structure is as a result of the underlying mobile shale which forms a diapiric structure as a result of sediment loading, thereby impacting or deforming the lithified sediments already deposited in the area. The impact of the shale diapirism is interpreted to be post-deformation, where sand deposition has been impacted by growing structure, hence, we a combination trap system.

The geometry (Fig. 12a) for the S1000 reservoir is such that channel type is interpreted to be weakly confined channel characterized by a straight pattern of channel axes and margin which were defined from amplitude maps. Overall, the channel covers an area of approximately 50 km^2 with variations in thickness from axes to margin.

The geometry (Fig. 13b) for the S2000 reservoir is such that channel type is interpreted to also typical of weakly confined channel complex, however, characterized by a less sinuous pattern compared to the S1000 reservoir. Dim amplitudes in between bright ones are interpreted to mud fill channels the channel axes and margin can be defined from amplitude maps; this is highly influenced by the diapiric structure. The distal and proximal areas are also defined. The crest of the structure of the S2000 reservoir is faulted and thickness of reservoir spreads towards the limb of the fold; overall, the channel covers an area of approximately 78.3 km^2. The geologic interpretation of the near-stack seismic amplitude is presented in Fig. 18a, b. This completely defines the Environment of Deposition (EOD); particularly,
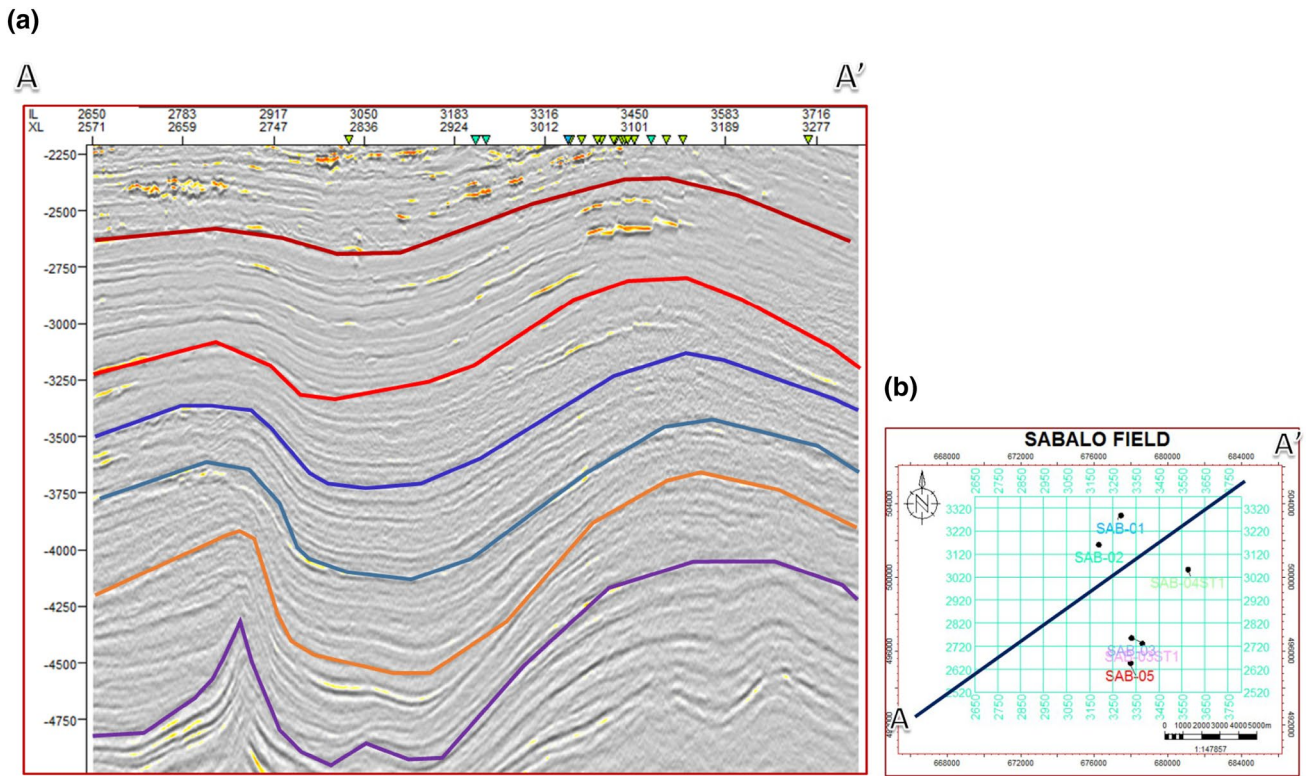
Fig. 17 Reservoir Geometry as a result of shale diapir. **a** Seismic section from A to A′ showing reflection geometry (the thick red lines are used to show dominant reflection geometry). **b** Base map of the study area showing the line of seismic section from A to A′
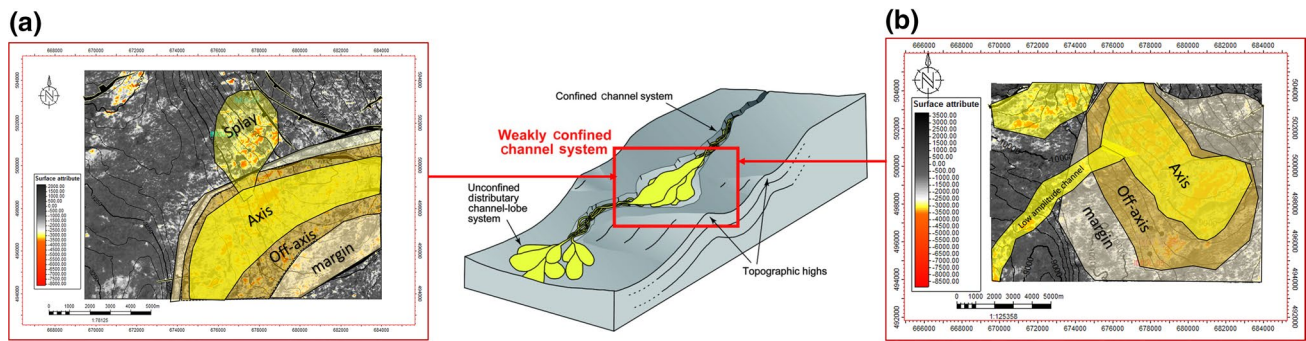

Fig. 18 Geological interpretation of near-stack amplitude extraction map. **a** S1000 reservoir top. **b** S2000 reservoir top

it clearly defines the division of the environment by showing the areas of channel axis, off-axis, margin and possible splay. This information is vital for reservoir development and management because there are good chances of getting a massive sand at the channel axis, hence, helping to provide target regions, and reduce risk of drilling into non-productive zones.

In terms of connectivity (In this case, static connectivity), S1000 is interpreted to be a loosely amalgamated system, while the S2000 is interpreted to be highly amalgamated. Seismic facies expression and analysis of log motifs (Figs. 12a and 13a) formed the basic from which connectivity was inferred. The S2000 is characterized by a high-amplitude channel axes comprise mostly massive, amalgamated sands. These characteristic helps improve connectivity within the reservoir.

Conclusion and recommendation

In summary, the outcome of our results indicates that the S2000 and S1000 reservoirs are more likely to be weakly confined channels, respectively. The S2000 covers an area of approximately 78 km^2 and the S1000 covers an area of approximately 50 km^2. The two reservoirs are both controlled structurally and stratigraphically and interpreted to be a combination trapping system. The S2000 has excellent qualities favouring hydrocarbon accumulation than the S1000 reservoir which has a fair quality. To further validate and retrieve more information about these reservoirs we recommend that spectral decomposition should be done to properly image the boundaries of channel axes, margins and splays.

References

Ahlbrandt TS, Charpentier RR, Klett TR, Schmoker JW, Schenk CJ, Ulmishek GF (2005) Global resource estimates from total petroleum systems. AAPG Mem. https://doi.org/10.1306/1061777M863175

Akindulureni JO, Adepelumi AA, Benjamin UK (2018) Evolution, geometry and formative processes of depositional elements in Niger Delta slope settings. Univ J Geosci 6(4):118–129

Alfaro E, Holz M (2014) Seismic geomorphological analysis of deepwater gravity-driven deposits on a slope system of the southern Colombian Caribbean margin. Mar Pet Geol 57:294–311

Amoyedo S, Atoyebi H, Bally J, Usman M, Nateganov A, Bergamo L, Berthet P (2016) Seismic-consistent reservoir facies modelling: a brown field example from deep water Niger Delta. In: SPE Nigeria annual international conference and exhibition. Society of Petroleum Engineers, Aug 2016

Bell JM, Chin YD, Hanrahan S (2005). State-of-the-art of ultra deepwater production technologies. In: Offshore technology conference, 2005 Jan. https://doi.org/10.4043/17615-MS

Bouma AH (1964) Turbidites. Dev Sedimentol. https://doi.org/10.1016/S0070-4571(08)70967-1

Bouma AH (2004) Key controls on the characteristics of turbidite systems. Geol Soc. https://doi.org/10.1144/GSL.SP.2004.222.01.02

Bouroullec R, Weimer P, Serrano O (2017) Regional structural setting and evolution of the Mississippi canyon, Atwater Valley, Western Lloyd Ridge, and Western Desoto Canyon protraction areas, northern deep-water Gulf of Mexico. AAPG Bull. https://doi.org/10.1306/09011609187

Brown AR (2011) Interpretation of three-dimensional seismic data. Society of Exploration Geophysicists and American Association of Petroleum Geologists, pp 103–156

Catuneanu O (2006) Principles of sequence stratigraphy. Elsevier, Amsterdam, pp 262–273

Chen J (2012) Understanding uncertainties in deepwater depositional facies modeling for better reservoir conditioning. In: SPE Europec/EAGE annual conference. Society of Petroleum Engineers

Deptuck ME, Sylvester Z (2018) Submarine fans and their Channels, Levees, and Lobes: In: Submarine geomorphology. Springer, Cham, pp 273–299. https://doi.org/10.1007/978-3-319-57852-1_15

Doust H (1990) Petroleum geology of the Niger Delta. In: Brooks J (ed) Classic petroleum provinces. Special Publications 501. Geological Society, London, p 365. https://doi.org/10.1144/GSL.SP.1990.050.01.21

Doust H, Omatshola E (1989) Niger Delta. In: Edwards JD, Santogrossi PA (eds) Divergent/passive margin basins: AAPG memoir, vol 48. American Association of Petroleum Geologists, pp 239–248

Evamy BD, Haremboure J, Kamerling P, Knaap WA, Molloy FA, Rowlands PH (1978) Hydrocarbon habitat of Tertiary Niger delta. AAPG Bull 62(1):1–39. https://doi.org/10.1306/C1EA47ED-16C9-11D7-8645000102C1865D

García M, Ercilla G, Alonso B, Estrada F, Jane G, Mena A, Alves T, Juan C (2015) Deep-water turbidite systems: a review of their elements, sedimentary processes and depositional models. Their characteristics on the Iberian margins. Boletín Geológico y Minero 126(2–3):189–218

Gath E (2011) Earth surface processes, landforms, and sediment deposits. Environ Eng Geosci. https://doi.org/10.2113/gseegeosci.17.1.92

Grahame J (2015) Deepwater Taranaki Basin, New Zealand—new interpretation and modelling results for Large Scale Neogene Channel and Fan Systems: implications for hydrocarbon prospectivity. In: AAPG/SEG 2015 international conference and exhibition (ICE), A powerhouse emerges: energy for the next fifty years. Sept 2015

Janocko M, Nemec W, Henriksen S, Warchoł M (2013) The diversity of deep-water sinuous channel belts and slope valley-fill complexes. Mar Petrol Geol 41:7–34

Jha P, Ros D, Kishore M (2011) Seismic and sequence stratigraphic framework and depositional architecture of shallow and deep-water Postrift sediments in East Andaman Basin: an overview. In: Conference: GEO-India 2011

Joye SB (2015) Deepwater Horizon, 5 years on. Science 349(6248):592–593. https://doi.org/10.1126/science.aab4133

Kahneman D, Tversky A (2013) Prospect theory: an analysis of decision under risk. In: Handbook of the fundamentals of financial decision making: Part I, pp 99–127. https://doi.org/10.1142/9789814417358_0006

Lanisa A (2010) Seismic facies analysis of tertiary deepwater slope deposits Lowers Congo Basin, Offshore Gabon. M.S. thesis, Royal Holloway, University of London, pp 52–68

Leduc AM, Davies RJ, Densmore AL, Imber J (2012) The lateral strike-slip domain in gravitational detachment delta systems: a case study of the northwestern margin of the Niger Delta. AAPG Bull 96(4):709–728

Leffler WL, Pattarozzi R, Sterling G (2011) Deepwater petroleum exploration & production: a nontechnical guide. PennWell Books, Tulsa

Lehu R, Lallemand S, Hsu SK, Babonneau N, Ratzov G, Lin AT, Dezileau L (2015) Deep-sea sedimentation offshore eastern Taiwan: facies and processes characterization. Mar Geol 369:1–18

Mitchum RM Jr, Vail PR, Thompson S III (1977) Seismic stratigraphy and global changes of sea level, Part 2: the depositional sequence as a basic unit for stratigraphic analysis. Seismic stratigraphy-applications to hydrocarbon exploration. Mem Am Assoc Petrol Geol 26:53–62

Moody JD, Pyles DR, Clark J, Bouroullec R (2012) Quantitative outcrop characterization of an analog to weakly confined submarine channel systems: Morillo 1 member, Ainsa Basin, Spain. AAPG Bull 96(10):1813–1841

Ndip EA, Agyingyi CM, Nton ME, Oladunjoye MA (2018) Seismic stratigraphic and petrophysical characterization of reservoirs of the Agbada formation in the vicinity of 'Well M'. Offshore Eastern Niger Delta Basin, Nigeria. J Geol Geophys 7(331):2

Obaje NG (2009) Geology and mineral resources of Nigeria, vol 120. Springer, New York. https://doi.org/10.1007/978-3-540-92685-6_10

Ofurhie MA, Lufadeju AO, Agha GU, Ineh GC (2002) Turbidite depositional environment in deepwater of Nigeria. In: Offshore technology conference, Jan 2002

Okpogo EU, Abbey CP, Atueyi IO (2018) Seismic facies analysis for lithofacies prediction, Okam Field of Niger Delta, Nigeria. Iraqi J Sci 59(3B):1430–1440

Olabode S, George U, Jihoon W, Olaoluwa I, Dolapo D (2010) Resolving the structural complexities in the deepwater Niger-Delta Fold and Thrust Belt: a case study from the Western Lobe, Nigerian Offshore Depobelt. Adapted from oral presentation at AAPG international conference and exhibition, Calgary, Alberta

Olubola A, Taiwo OM (2016) Seismic facies analysis and depositional process interpretation of 'George Field', Offshore Niger Delta, Nigeria. J Basic Appl Res Int 13:243–252

Posamentier HW, Kolla V (2003) Seismic geomorphology and stratigraphy of depositional elements in deep-water settings. J Sediment Res 73(3):367–388. https://doi.org/10.1306/111302730367

Quiquerez A, Sarih S, Allemand P, Garcia JP (2013) Fault rate controls on carbonate gravity-flow deposits of the Liassic of Central High Atlas (Morocco). Mar Petrol Geol 43:349–369. https://doi.org/10.1016/j.marpetgeo.2013.01.002

Reader TW, O'Connor P (2014) The Deepwater Horizon explosion: non-technical skills, safety culture, and system complexity. J Risk Res 17(3):405–424

Rider M (1999) Geologic interpretation of well logs. Whittles Publishing Services, pp 226–229

Shanmugam G (2013) New perspectives on deep-water sandstones: implications. Petrol Explor Dev 40(3):316–324

Simm R, Bacon M, Bacon M (2014) Seismic Amplitude: an interpreter's handbook. Cambridge University Press, Cambridge

Skogdalen JE, Vinnem JE (2012) Quantitative risk analysis of oil and gas drilling, using Deepwater Horizon as case study. Reliab Eng Syst Saf 100:58–66. https://doi.org/10.1016/j.ress.2011.12.002

Sprague ARG, Garfield TR, Goulding FJ, Beaubouef RT, Sullivan MD, Rossen C, Campion KM, Sickafoose DK, Abreu V, Schellpeper ME, Jensen GN (2005) Integrated slope channel depositional models: the key to successful prediction of reservoir presence and quality in offshore West Africa. In: Conference: CIPM, Veracruz

Stacher P (1995) Present understanding of the Niger Delta hydrocarbon habitat. In: Oti MN, Postma G (eds) Geology of Deltas. AA Balkema, Rotterdam, pp 257–267

Tari GC, Simmons MD (2018) History of deepwater exploration in the Black Sea and an overview of deepwater petroleum play types. In: Simmons MD, Tari GC, Okay AI (eds) Petroleum geology of the Black Sea. Geological Society Special Publication No. 464. Geological Society, London, pp 439–475

Vail P (1977) Seismic stratigraphy and global changes of sea-level, part 4: global cycles of relative changes of sea-level. Seismic stratigraphy-applications to hydrocarbon exploration. Mem Am Assoc Petrol Geol 26:83–98

Veeken PC (2006) Seismic stratigraphy, basin analysis and reservoir characterisation, vol 37. Elsevier, Amsterdam

Whiteman AJ (2012) Nigeria: its petroleum geology, resources and potential, vol 1. Springer, New York

Widess MB (1973) How thin is a thin bed? Geophysics 38(6):1176–1180. https://doi.org/10.1190/1.1440403

Xu ZC, Ma HX, Fan GZ, Lu FL, Ding LB (2016) Deep water depositional architecture, evolution and reservoir potential in the Rakhine Basin, Offshore Myanmar. In: 78th EAGE conference and exhibition 2016

Zhang L, Pan M, Wang H (2017) Deepwater turbidite lobe deposits: a review of the research frontiers. Acta Geologica Sinica (English Edition) 91(1):283–300

Publisher's Note Springer Nature remains neutral with regard to jurisdictional claims in published maps and institutional affiliations.